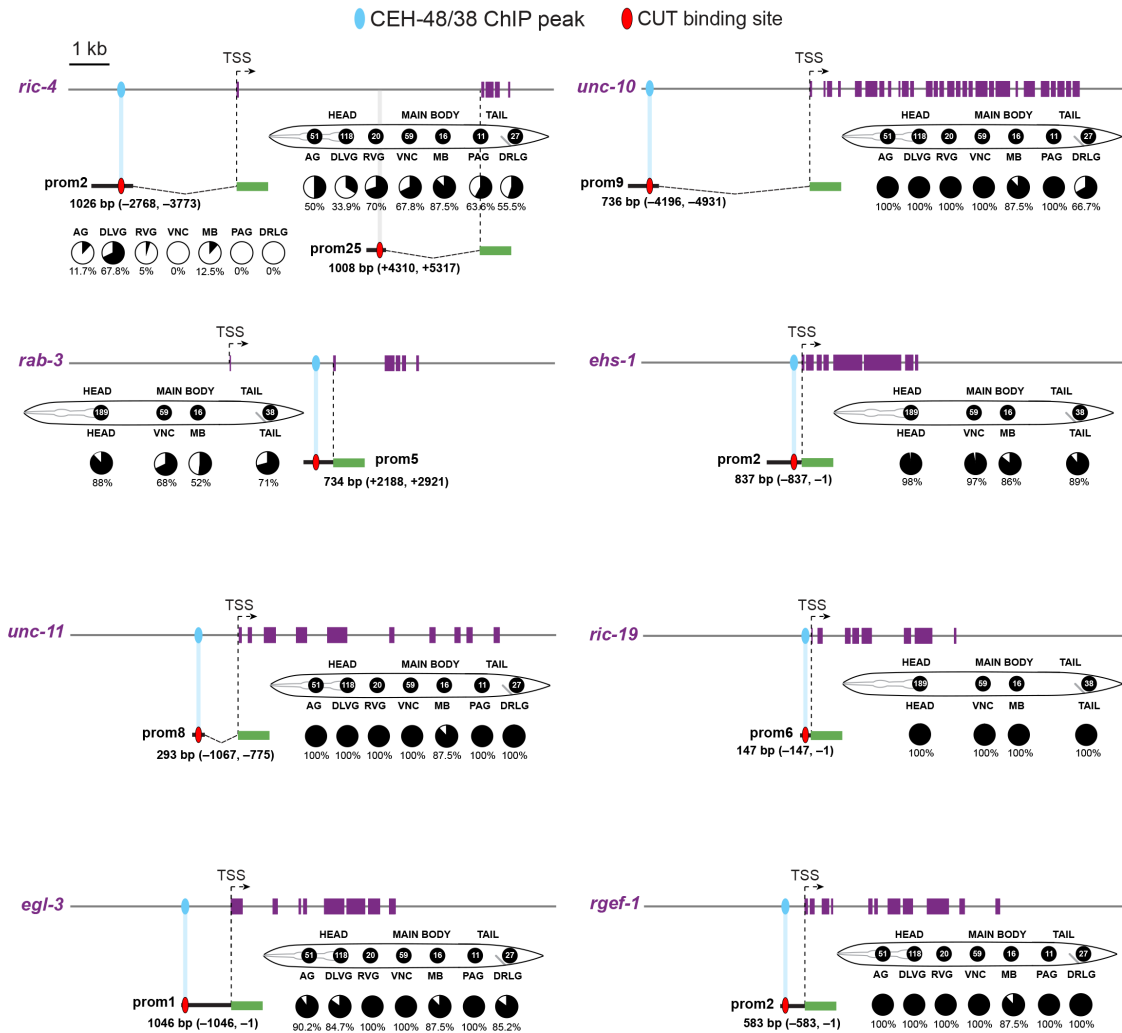


**Figure S1. Comparison of the expression level of CUT genes. Related to Figure 1.**

Expression of *ceh-38*(*syb4799*[*ceh-38::GFP*]), *ceh-48*(*ot1125*[*ceh-48::GFP*]), *ceh-44*(*ot1015*[*ceh-44::GFP*]) and *ceh-41*(*syb4901*[*ceh-41::GFP*]) CRISPR/Cas9-engineered *gfp*-tagged alleles. Lateral views of the worm head at the L4 stage are shown. Quantification of reporter allele fluorescence intensity in nerve ring neurons (outlined). The data are presented as individual values with each dot representing the expression level of one worm with the mean  $\pm$  SEM indicated. One-way ANOVA followed by Tukey's multiple comparisons test; \*\*\* $P < 0.001$ .  $n \geq 10$  for all genotypes. a.u., arbitrary units. Scale bar 15  $\mu$ m.



**Figure S2. Pan-neuronal *cis*-regulatory elements are bound by CUT factors. Related to Figure 2.**

CUT ChIP binding correlates with the *cis*-regulatory elements that we previously defined in pan-neuronally expressed genes<sup>S1</sup>. Schematic representation of *ric-4*, *unc-10*, *rab-3*, *ehs-1*, *unc-11*, *ric-19*, *egl-3* and *rgef-1* gene loci. For each gene, a schematic representation of the nervous system of *C. elegans* is shown. Neurons belonging in the different ganglia or regions, are clustered together and represented by a black circle (number of neurons belonging in each ganglion are indicated inside the circle). Below each worm schematic, the fraction of neurons of each ganglion expressing a reporter is indicated with a partially filled circle

(pie-chart). Promoter fragment gene fusion reporters expression data from <sup>S1</sup>. For *ric-4*, mutation of the CUT homeodomain binding site (site 1) overlapping the ChIP peak had no effect on the expression of a *ric-4* CRISPR reporter (**Figure 2C and E**). We made use of our previous *ric-4* cis-regulatory analysis <sup>S1</sup> to guide our search for CUT homeodomain binding sites within cis-regulatory elements driving broad neuronal expression. We found a cluster of CUT homeodomain binding sites (site 2) in the previously defined *ric-4* promoter fragment 25 (prom25), located within the first *ric-4* intron. Upon mutation of this cluster, together with site 1, we found a reduction on *ric-4* CRISPR reporter expression (**Figure 2C and E**). AG: anterior head ganglion; DLVG: dorsal, lateral, and ventral head ganglia; RVG: retrovesicular ganglion; VNC: ventral nerve cord motor neurons; MB: mid-body neurons; PAG: preanal ganglion; DRLG: dorsorectal and lumbar ganglia. The length in bp and the coordinates of each promoter fragment in relation to the translational start site are shown next to each construct. Promoter fragment number corresponds to the cis-regulatory analysis generated in <sup>S1</sup>.

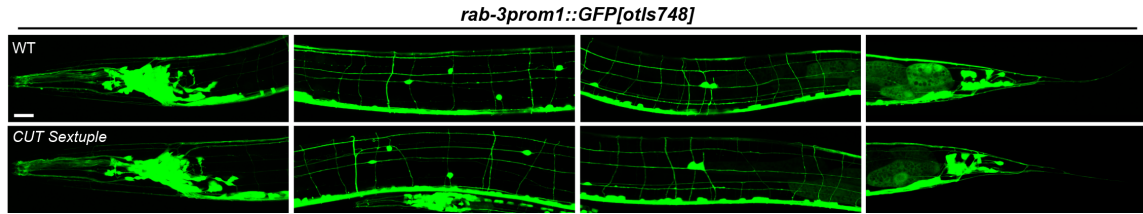


**Figure S3. Overall neuronal anatomy is not affected in CUT gene mutant.**

**Related to Figure 4.**

Overall nervous system anatomy (visualized through a *rab-3* cytoplasmic reporter, *rab-3prom1::GFP[otIs748]*) is not affected in CUT sextuple mutant (bottom) when compared to wild-type (top) animals. All images correspond to worms at the L4 larval stage. Signal is shown saturated in both genotypes to visualize the axonal tracts, therefore the defect on *rab-3* expression in the CUT sextuple mutant is not visible here.

WT, wild-type; Scale bar 15  $\mu$ m.

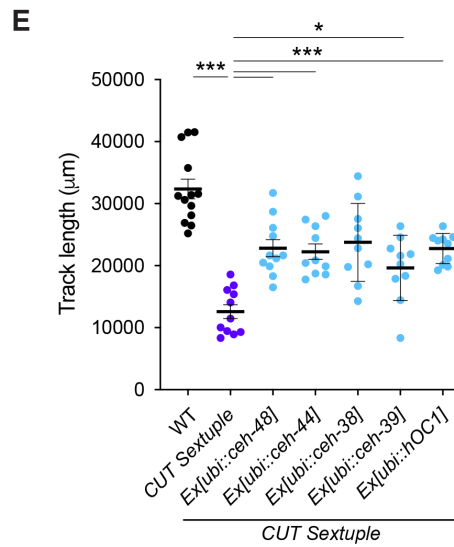
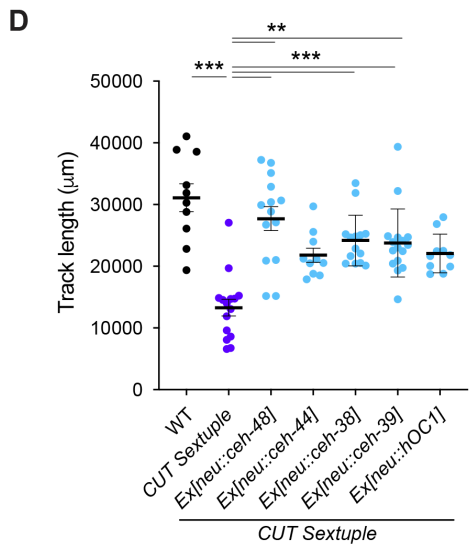
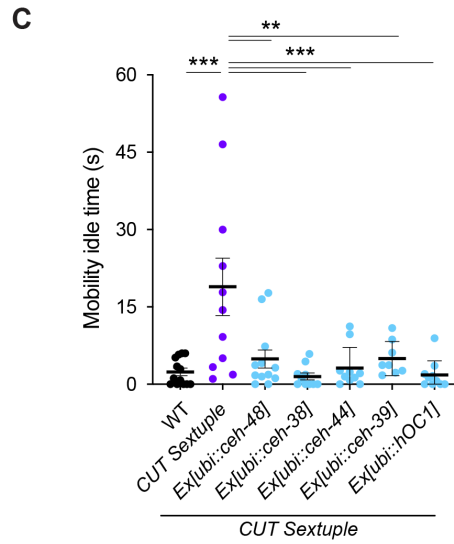
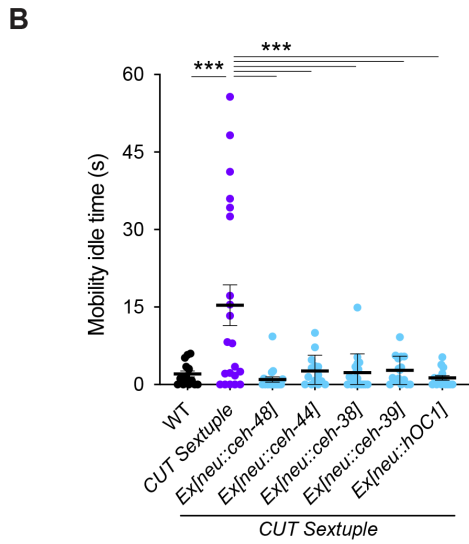
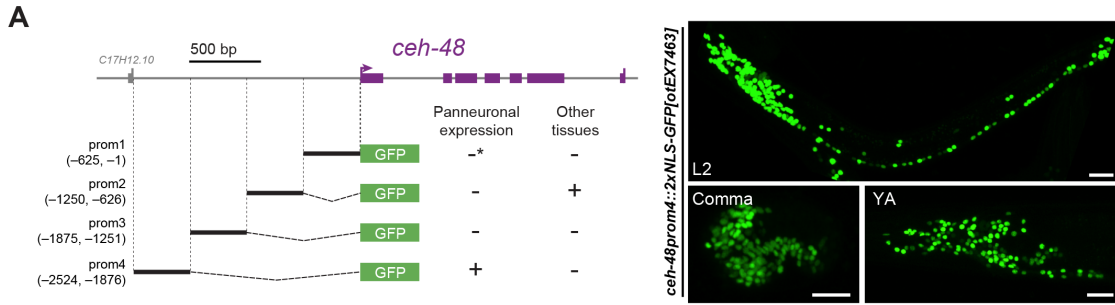


**Figure S4. *ceh-48* cis-regulatory analysis and rescue of locomotion phenotypes in CUT sextuple mutants. Related to Figure 3 and Figure 4.**

**(A)** Promoter fragment 4 (*prom4*) is expressed pan-neuronally and was used to drive pan-neuronal expression in the rescue lines. Promoter fragment 1 (*prom1*) is expressed in some midbody neurons (asterisk). Promoter fragment 2 (*prom2*) is expressed in some vulval cells. Expression of a *prom4* fusion to GFP (right) is shown at the comma embryonic stage (bottom left, lateral view), L2 larval stage (top, full worm lateral view) and young adult stage (bottom right, lateral view of the head) showing *ceh-48prom4::2xNLS-GFP[otEX7463]* pan-neuronal expression.

**(B-E)** Worm mobility idle time (**B-C**) and track length (**D-E**) was compared between wild-type, CUT sextuple mutant, and CUT sextuple mutant rescue (panneuronal, *ceh-48* promoter (“neu”) (**B and D**), or ubiquitous, *eft-3* promoter (“ubi”) (**C and E**), expression of *ceh-48*, *ceh-44*, *ceh-38*, *ceh-39* or *hOC1*) using a multi-worm tracker system<sup>S2</sup>. The data are presented as individual values with each dot representing the value of one worm with the mean  $\pm$  SEM indicated. One-way ANOVA followed by Tukey’s multiple comparisons test, comparisons with CUT sextuple mutant indicated; \*P < 0.05, \*\*P < 0.01, \*\*\*P < 0.001. n  $\geq$  10 for all genotypes.

YA, young adult; WT, wild-type; Scale bar 15  $\mu$ m.

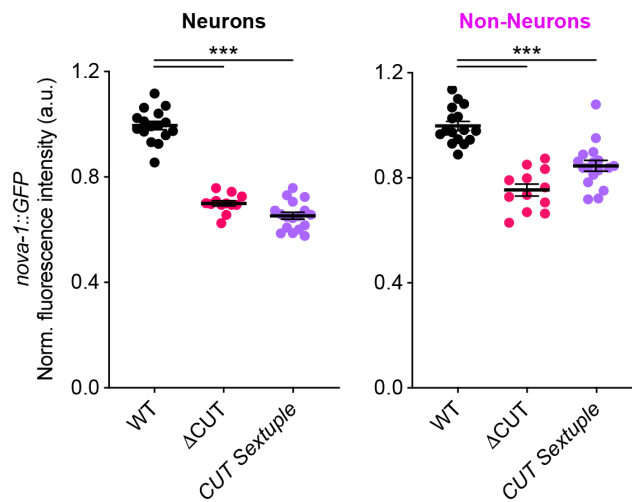
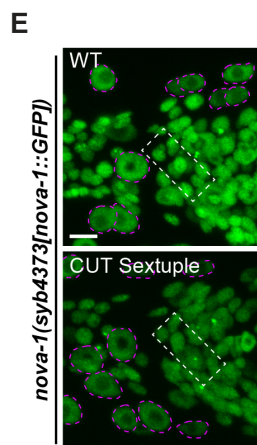
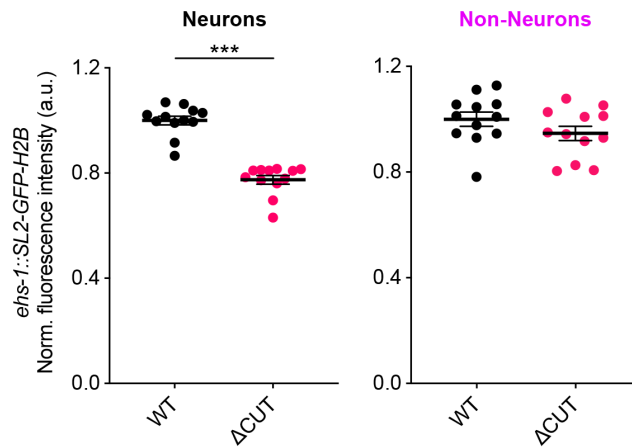
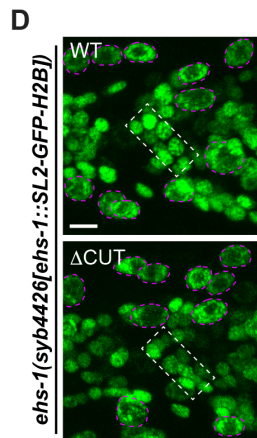
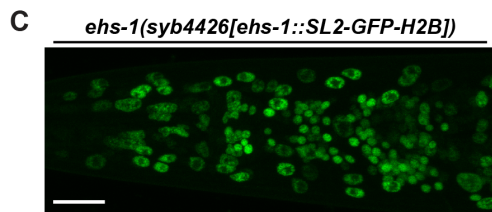
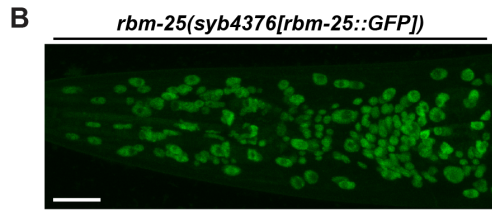
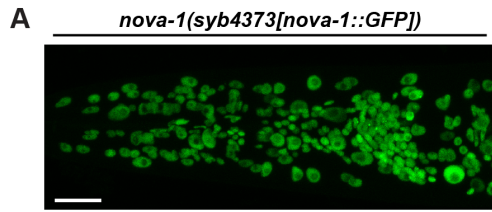


**Figure S5. CUT genes regulate some ubiquitously expressed genes with neuronal functions. Related to Figure 5.**

(A-C) Expression of *nova-1*(*syb4373[nova-1::GFP]*) (A), *rbm-25*(*syb4376[rbm-25::GFP]*) (B) and *ehs-1*(*syb4426[ehs-1::SL2-GFP-H2B]*) (C) CRISPR/Cas9-engineered *gfp*-tagged alleles in wild-type animals. These genes are downregulated in the CUT sextuple mutant transcriptional analysis (*ehs-1* is just above the significant threshold in the DESeq2 analysis, adjusted p-value = 0.070, p-value = 0.015).

(D) CUT homeodomain binding site mutation in the *ehs-1* endogenous promoter (bottom) causes a reduction on *ehs-1* expression in neurons compared to wild-type (top), but not in non-neuronal cells. Lateral views of the worm head at the L4 stage are shown. Quantification of *ehs-1*(*syb4426[ehs-1::SL2-GFP-H2B]*) fluorescence intensity in nerve ring neurons (white outlined box) and head epidermal cells (outlined in magenta). The data are presented as individual values with each dot representing the expression level of one worm with the mean  $\pm$  SEM indicated.

Unpaired *t*-test, \*\*\*P < 0.001. n = 12 for all genotypes.

(E) Expression of *nova-1*(*syb4373[nova-1::GFP]*) in wild-type (top) and CUT sextuple mutant (bottom). Lateral views of the worm head at the L4 stage are shown. Quantification of *nova-1*(*syb4373[nova-1::GFP]*) fluorescence intensity in nerve ring neurons (white outlined box) and head epidermal cells (outlined in magenta) in wild-type, CUT sextuple mutants and upon CUT homeodomain binding site mutation in the regulatory control regions of *nova-1* ( $\Delta$ CUT: *nova-1*(*syb4373 syb5446*)). The data are presented as individual values with each dot representing the expression level of one worm with the mean  $\pm$  SEM indicated.

One-way ANOVA followed by Tukey's multiple comparisons test, \*\*\*P < 0.001. n  $\geq$  12 for all genotypes

WT, wild-type; a.u., arbitrary units. Scale bars 15  $\mu$ m (A-C), 5  $\mu$ m (D-E).



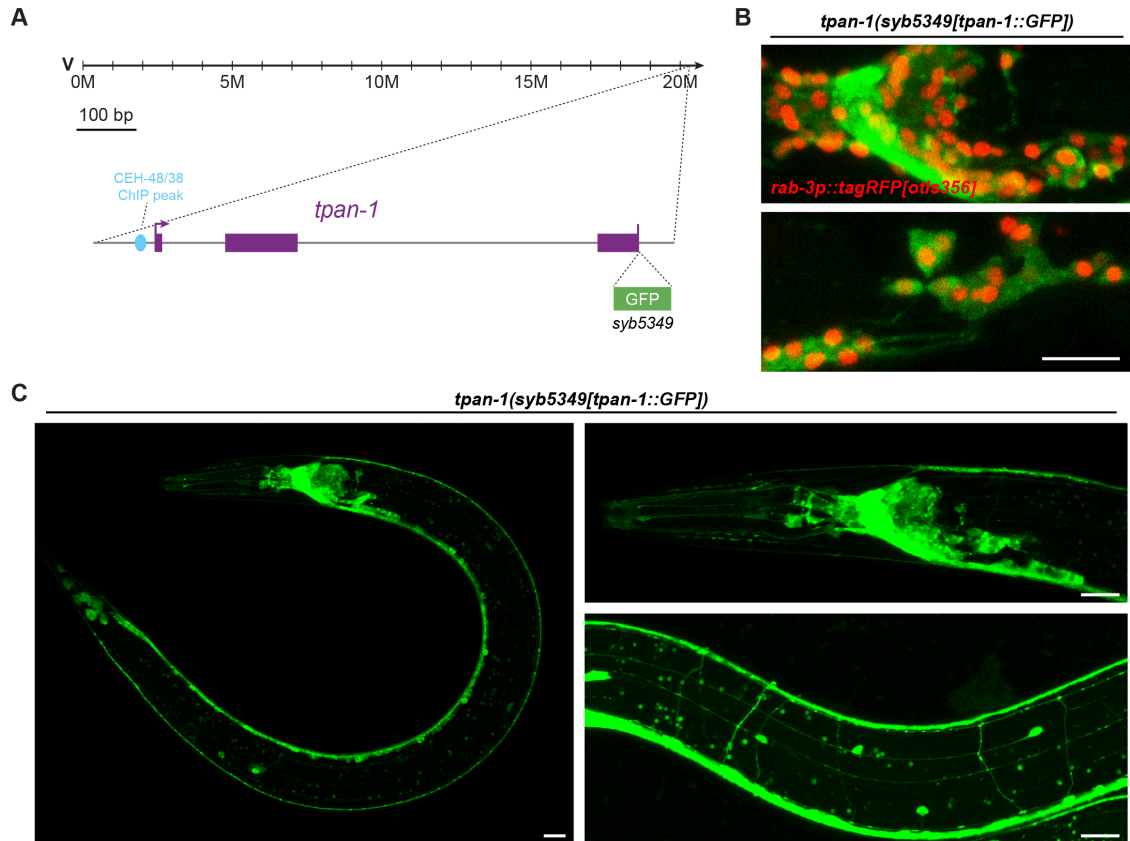


**Figure S6. *tpan-1* is a novel CUT gene target expressed pan-neuronally.**

**Related to Figure 5.**

(A) Schematic representation of *tpan-1* gene locus showing the location of the CEH-48/CEH-38 ChIP peaks and GFP tag.

(B) *tpan-1* CRISPR reporter (*tpan-1(syb5349[tpan-1::GFP])*) expression overlaps with the nuclear pan-neuronal marker *rab-3prom1::2xNLS-tagRFP[otIs356]*. Most of the TPAN-1::GFP signal is clustered in the nerve ring bundle, consistent with its cytoplasmic localization.

(C) *tpan-1* CRISPR reporter (*tpan-1(syb5349[tpan-1::GFP])*) expression overview (left) and cytoplasmic expression seen in soma and neuronal projections (right). Note in the bottom right panel that all major fascicles show TPAN-1::GFP expression, consistent with a pan-neuronal nature of *tpan-1* expression.

YA, young adult. Scale bars 15  $\mu$ m.

## SUPPLEMENTAL REFERENCES

- S1. Stefanakis, N., Carrera, I., and Hobert, O. (2015). Regulatory Logic of Pan-Neuronal Gene Expression in *C. elegans*. *Neuron* 87, 733-750. [10.1016/j.neuron.2015.07.031](https://doi.org/10.1016/j.neuron.2015.07.031).
- S2. Roussel, N., Sprenger, J., Tappan, S.J., and Glaser, J.R. (2014). Robust tracking and quantification of *C. elegans* body shape and locomotion through coiling, entanglement, and omega bends. *Worm* 3, e982437. [10.4161/21624054.2014.982437](https://doi.org/10.4161/21624054.2014.982437).